MODELLING 2D AND 3D SEPARATION FROM CURVED SURFACES WITH ANISOTROPY-RESOLVING TURBULENCE CLOSURES

C. Wang, Y.J. Jang and M.A. Leschziner
Department of Aeronautics,
Imperial College London,
South Kensington, London SW7 2AZ, UK
Mike.leschziner@imperial.ac.uk

ABSTRACT

The ability of non-linear eddy-viscosity and second-moment models to predict separation from two-and three-dimensional curved surfaces is examined by reference to two flows that are geometrically akin: one separating from periodically-spaced two-dimensional 'hills' in a plane channel, and the other from a three-dimensional hill in a duct. One major objective is to examine whether the predictive performance in 3-d conditions relates to that in 2d flow. In the former, the separation pattern is far more complicated, being characterised by multiple vortical structures associated with 'open' separation. The predicted separation behaviour in the 2-d flow differs significantly from model to model, with only one non-linear model among those examined performing well, this variant formulated to adhere to the two-component wall limit. In 3-d separation, none of the models gives a credible representation of the complex multi-vortical separation pattern.

INTRODUCTION

Separation from curved surfaces is one of the hardest aerodynamic processes to predict correctly. Yet, it is the key to determining the gross flow properties in and the operational performance of a wide variety of engineering devices, especially in aero-mechanical engineering.

A major predictive challenge arising in this respect is that even slight changes in the time-averaged location of the separation line are observed to result in substantial changes in the reattachment behaviour and thus in gross-flow features. The fundamental problem of 'non-locality' aside, the time-mean separation process can be expected to depend sensitively on the evolution of the boundary layer as it decelerates and skews, the latter in 3-d, while subjected to adverse pressure gradient. This is an important difference relative to separation from a sharp corner. In terms of statistical properties, the separation behaviour depends on the differentiated response of the turbulent stresses in the boundary layer to shear, irrotational and curvature-related straining, and turbulence anisotropy is likely to play an important role in this response. Similarly complex interactions are effective in the separated, curved shear layer, in the intense streamwise vortices in 3d, in the reattachment process and in the post-reattachment-recovery region.

Much effort has gone into the investigation of turbulence closures more complex than linear eddy-viscosity models for separated flows, although rarely in conditions in which separation from a continuous surface is provoked by the action of a moderate adverse pressure gradient. Several studies have examined the predictive performance of a range of non-linear eddy-viscosity, explicit algebraic Reynolds-stress and full second-moment models for separated laboratory flows in an effort to identify optimal modelling methodologies (e.g. Lien & Leschziner (1995,1997), Apsley & Leschziner (2000), Hanjalic (1994), Craft (1998), May (1999), Jang et al (2003)). Moreover, a number of collaborative efforts, notably recent workshops organised under the auspices of ERCOFTAC (Rodi et. al (1998), Jakirlic (2001)) have included key test cases that feature separation from curved surfaces. Most of this work has been undertaken within a 2-d framework, because of the relatively modest computational effort involved, the more abundant availability of experimental data and the promise of greater insight into fundamental issues. Although suggesting that significant predictive advantages can be derived from anisotropy-resolving models in some cases, model performance has been observed to be uneven, and some of the studies involve uncertainties arising from insufficient data and 3d contamination of the experimental flow or other experimental limitations. A crucially important open question is whether the conclusions derived for 2D conditions translate to 3-d flows. Some encouraging indications are provided by the studies of Lien & Leschziner (1997) and Apsley & Leschziner (2000), but both involve flow-specific limitations and do not suffice to draw firm conclusions. There is, therefore, a strong need to broaden the range of 3-d flows investigated. The outcome of such investigations will, in effect, dictate whether elaborate closures will be adopted more widely for complex practical applications.

This paper focuses on two related flows featuring separation from curved surfaces, one 2-d and the other 3-d, both shown in Fig. 1. The former geometry is a nominally infinite sequence of periodic 2-d 'hills' in a channel at Re=21200, based on mean velocity and channel height. Extensive data for spanwise homogeneous and streamwise periodic flow conditions are available for this case from highly-resolved LES computations by Temmerman et. al. (2003). The 3-d geometry is a circular hill (in plan) placed on the lower wall of a duct. Its cross-section is similar in shape to that of the 2-d hill. The flow around it, at Reynolds number 130000, based on hill

height and free-stream velocity, was investigated experimentally by Simpson and Long (2002) using LDV. It features a complex, multi-vortical separation pattern in the leeward side of the hill, as shown in Fig. 1. Thus, although the 2-d and 3-d flows are geometrically akin, the latter is physically much more complex than the former.

The 2-d flow, treated as a single periodic hill-crest-to-hill-crest segment, has been the subject of a recent study by Jang et al (2003), which examined the performance of a range of non-linear eddy-viscosity and explicit algebraic Reynolds-stress models. An issue addressed in this paper in relation to this flow is whether streamwise periodicity is an important aspect in judging alternative turbulence closures. Periodicity is often said to be unrepresentative of real predictive situations and assumed to pose added challenges by the fact that errors in the inner-domain solution are fed back to the inlet plane, thus progressively amplifying the departure of the model solution from reality and obscuring model capabilities. The extent to which this issue affects conclusions on closure performance and their applicability to cases in which the inlet flow is specified as a boundary condition is addressed by performing computations for a sequence of 3 hills, with LES conditions applied to the inflow plane, as well as for a single segment, with imposed periodicity conditions. The former practice allows the rate of approach to the periodic state to be studied and the 'anchoring' influence of the specified inlet conditions to be identified in terms of its importance to the assessment of turbulence models.

TURBULENCE MODELS

Four turbulence models are investigated herein, namely: the Apsley-Leschziner (1998) cubic eddy-viscosity model (AL-ε); the Wallin-Johansson (2000) explicit algebraic stress model (WJ-ω); the Abe-Jang-Leschziner quadratic eddy-viscosity model (2003) (AJL-ω); and the Speziale-Sarkar-Gatski Reynolds-stress transport model (1991), extended to low-Re conditions by Chen (1995) (SSG-ε), in which the extensions 'ε' and 'ω' to the abbreviations indicate the nature of the length-scale equation used in the models. This is a selection from a broader investigations including further non-linear eddy-viscosity and Reynolds-stress models (NLEVMs and RSTMs). The selected group contains a representative cubic model (derived by from simplified Reynolds-stress model), the most recent explicit algebraic Reynolds-stress model, (quadratic in 2-d and quartic in 3-d), a representative Reynolds-stress-transport model and a recently formulated quadratic model formulated to adhere to the correct limiting behaviour of near-wall turbulence (see below). The above selection may be claimed to represent the two principal groups of anisotropy-resolving turbulence models currently considered as primary alternatives to isotropic-viscosity models for complex flow applications. More advanced forms second-moment closure exist (eg. Jakirlic & Hanjalic (1995), Craft and Launder (1996), Batten et al (1999)). However, experience suggests that their predictive performance in complex flow conditions is not fundamentally different from that of simpler second-moment closures.

The quadratic low-Re model of Abe et al (AJL-ω) is new and differs in two important respects from other models of the NLEVM type. First, it augments the basic quadratic constitutive stress-strain/vorticity equation by two additive fragments intended to account, respectively, for high normal straining and strong near-wall anisotropy. Second, it uses a form of the ω-equation that is much closer than Wilcox's form to the ε-equation. Specifically, it includes products of k and ω gradients and coefficients for the production and destruction terms that are directly equivalent to $C_{\varepsilon 1}$ and $C_{\varepsilon 2}$ normally used in the ε-equation.

An influential additive model fragment accounts specifically for strong near-wall anisotropy and for the correct decay towards two-component turbulence that is observed in DNS. This decay cannot be represented solely by the use of terms combining the strain and vorticity, and there is a need to introduce a tensorially correct term that takes into account the wall orientation. In the model variant used here, the wall-direction indicator is:

$d_i = N_i / \sqrt{N_k N_k}$, $N_i = \partial l_d / \partial x_i$, $l_d = y_n$ (wall distance)

which is then used in the wall-anisotropy correction,

$$ {}^{w}a_{ij} = -f_w \left(d_i d_j - \frac{\delta_{ij}}{3} d_k d_k \right) $$

with f_w being a viscosity-related damping function. Alternative wall-orientation indicators that are independent of wall distance may readily be used. In the above damping function, a composite time scale is used, which combines the macro-scale k/ε with the Kolmogorov scale $\sqrt{\nu/\varepsilon}$. The damping function f_w then provides a smooth transition between the two scales across the near-wall layer.

COMPUTATIONAL ISSUES

Numerical Procedure

Computations were performed with a non-orthogonal, collocated, cell-centred finite-volume approach implemented in the code 'STREAM' (Lien and Leschziner (1994), Apsley and Leschziner (2000)). Convection of both mean-flow and turbulence quantities is approximated by the 'UMIST' scheme (Lien and Leschziner (1994)) - a second-order TVD approximation of the QUICK scheme. Mass conservation is enforced indirectly by way of a pressure-correction algorithm. Within this scheme, the transport and the pressure-correction equations are solved sequentially and iterated to convergence.

2-d hill flow

Previous computations by Jang et al (2003) have treated this flow as perfectly period. Here, in contrast, a sequence of three hills is considered for reasons explained in the introduction. Inlet conditions, taken from the LES solution, were specified 2 hill heights upstream of the first hill, a position at which the flow undergoes recovery from the reattachment 2.5 hill heights further upstream. Following grid-dependence tests, a non-uniform grid

comprising 90x700 nodes has been used. The grid is compressed towards the walls, with 5 nodes covering the viscous sublayer down to y^+=0.5. The channel following the third hill is extended to allow the flow to recover to a state allowing zero-streamwise-gradient conditions to be prescribed with little error. Although the hill-to-hill distance allows for a significant length of post-reattachment recovery, the above practice poses some (probably minor) uncertainty in terms of the influence of any downstream hill on the separated flow upstream of that hill.

3-d hill

The hill stands on the lower wall of a sufficiently large duct to be only subjected to the lower-wall boundary layer. The thickness of this layer 2 hill-heights upstream of the hill is approximately 0.5 hill heights. Measurements for this case are available, in the form of profiles of mean-flow, Reynolds-stresses and their orientation, at 3.7 hill-heights downstream of the hill crest. In addition, hill-topology results are reported. Unfortunately, no upstream conditions are available, so that the inlet flow cannot be specified directly. Instead, profiles of velocity and Reynolds-stresses have been measured in the duct *with the hill removed* at the location corresponding to the hill top. To generate inlet conditions, pre-curser hill-free duct calculations were performed over a length 20 hill heights, and the reference hill-top location was determined by matching the solution to the measured duct-flow profiles. The result of this matching process is indicated in Fig. 2 for 3 models. The conditions returned by the solution 4 hill heights upstream of the matching location were then taken as inlet conditions for the hill calculations. The sensitivity to errors in the matching process was then investigated by repeating some hill computations with inlet conditions taken at 1 hill height upstream and downstream of the reference location.

RESULTS

2-d hill

Profiles of streamwise velocity and Reynolds shear stress at x/h=2, predicted by the four models outlined earlier, are shown in Fig. 3 and Fig. 4, respectively. Each plot contains five profiles: one the reference LES solution, one the period solution reported by Jang et al (2003), and three profiles relating to the conditions after the first, second and third hill, respectively. Fig. 5 provides plots of streamfunction contours for the flow between the second and third hills, and below them, related plots showing how the reattachment location changes as the flow progresses from the first to the second and third hill. The hill-to-hill variation in reattachment location in compared with that returned by the periodic and LES solutions, both represented by related horizontal lines, identifying hill-independent values.

Fig. 5 demonstrates the degree to which the imposition of periodicy does or does not impact on the assessment of models' predictive characteristics. It can be argued that streamwise periodicity is unrepresentative of practical problems in which the prescribed upstream conditions tend to 'anchor' the solution, so that model defects are understated, while defects are amplified by the feedback mechanism inherent in the imposition of periodicity. The present results contradict this argument. As seen, a model returning a periodic solution that is relatively far from the correct one (e.g. WJ-ω) also gives large errors in the non-periodic implementation. Indeed, the error is initially larger, settling – as must be the case – to that of the periodic implementation. The profiles in Figs. 3 and 4 show that the main predictive characteristics of a model are well established after the first hill, and that only relatively minor changes in the flow structure occur as the flow progresses downstream. Self-evidently, this is especially so in the case of a model that gives a periodic solution that is close to the baseline LES field. This applies, in particular, to the Abe-Jang-Leschziner model that is shown by in Jang et al (2003) to give the best representation of the flow and also performs well in a-priori tests based on the LES fields. Despite this generally favourable predictive quality, Fig. 4 shows that even this model returns insufficient shear stress in the separated shear layer – a defect common to all models and probably reflecting large-scale unsteadiness in the separation location, discussed in the introduction. Of the models examined, that by Wallin and Johansson (WJ-ω) does least well, giving a seriously excessive separation length, possibly because of the particular form of the ω-equation it uses. The SSG-ε performs almost as badly, the characteristic doubling up of the separation streamline close to reattachment hiding, to some extent, the exaggerated separation region.

3-d hill

The principal experimental data available for this case are velocity and Reynolds-stress profiles 3.7 hill heights downstream of the hill crest. Derived from these are further data for the parameters $SSA = \tan^{-1}\left(-\overline{vw}/-\overline{uv}\right)$ and $S^{-1} = \sqrt{\left(-\overline{uv}\right)^2 + \left(-\overline{vw}\right)^2}\Big/\overline{vv}$. Additional surface data include oil-film traces on the hill surface and a skin-friction distribution on the lower wall, again at 3.7 hill heights downstream of the hill crest.

Fig. 6 compares predicted skin-friction (or limiting streamlines) on the hill surface with a topological map extracted from the oil-film experiments, the former being a somewhat stylised representation of latter, which is not symmetrical about the hill's centre-plane. As is evident, there are major differences between all model predictions and the experiment. The latter shows footprints of three distinct vortex pairs, while the models all predict a single pair associated with a single separation line on the hill's leeward side. The four 'particle' traces shown in Fig. 7 – some of numerous examined – are consistent with Fig. 6, in so far as they confirm the existence of a single pair of intense vortices. The upstream origins of the traces are identical for all models, and their downstream evolution indicates not insignificant differences between the predicted vortex structure. One major consequence of the

structural differences is a much more intense wake predicted by the calculations in comparison with reality (Fig. 8). Another consequence, associated with the existence of a distinctive node 'N_s' in the experimental topology map at the rear foot of the hill (Fig. 6), is that the experimental near-wall flow diverges beyond the hill, while the computed flow converges towards the centre-plane. Fig. 8 shows wall-normal profiles of velocity and turbulence energy at various spanwise locations predicted with the AJL-ω and the SSG-ε models. The solutions the other two models yield are qualitatively similar to that arising from AJL-ε model. The profiles demonstrate that the computed wake is far too intense and confined to a much too small spanwise portion around the centre-plane. Consistently, the skin-friction-magnitude, Fig. 9, varies too rapidly in the region $0<z/H<3$. Note, however, the extent of asymmetry in the experimental data. Comparisons for the parameter S^{-1} have been included here for the principal purpose of examining the near-wall behaviour of the stresses. It is recalled that the AJL model is designed to return the correct wall-asymptotic behaviour. This is confirmed in Fig. 8, albeit qualitatively, by the sharp rise in S^{-1} as the wall is approached. The Reynolds-stress closure returns a qualitatively similar behaviour, but is not specifically formulated to give the correct near-wall decay of the stresses.

The general behaviour observed above, especially in Fig. 8, is reminiscent of that returned by other RANS computations around bluff bodies, in which large-scale coherent unsteady features associated with shedding are not resolved, hence displaying substantially too low broadening of the time-averaged wake. In the light of this observation, first unsteady RANS computations have now been performed, but these have so far failed to yield unsteady features.

CONCLUSIONS

A computational study has been undertaken to examine the ability of anisotropy-resolving turbulence models to predict 2-d and 3-d separation from curved surfaces forming hill-shaped obstructions.

In the 2-d case, most models of this ilk over-estimate the size of the recirculation. This is associated with an insufficient level of the shear stress in the separated shear layer. An exception, in a number of respects, is the non-linear EVM model by Abe et al. This has been shown here, as was done in an earlier study on a periodic segment, to give results quite close to the LES solution. The present study has shown that the imposition of periodicy does not impact on the conclusions derived earlier: the present computations encompassing three hills with prescribed inlet conditions show that a model performing poorly in periodic conditions performs (or at least may perform) even more poorly with prescribed inlet conditions.

Disappointingly, none of the models examined gives a satisfactory representation of the corresponding 3-d separation process. The computations appear to miss some important mechanisms that are responsible for a multiple-vortex structure in the wake. Whether this is due to large-scale dynamics being missed is an issue which remains to be resolved, probably be means of Large Eddy Simulation.

ACKNOWLEDGEMENTS

The authors are grateful to the UK Engineering and Physical Sciences Research Council, BAE Systems and the EU for their financial support of different parts of the research report herein, The EU-funded work was undertaken within FLOMANIA (Flow Physics Modelling – An Integrated Approach), a collaboration between Alenia, AEA, Bombardier, Dassault, EADS-CASA, EADS-Military Aircraft, EDF, NUMECA, DLR, FOI, IMFT, ONERA, Chalmers University, Imperial College, TU Berlin, UMIST and St. Petersburg State University. The project is funded by the European Union and administrated by the CEC, Research Directorate-General, Growth Programme, under Contract No. G4RD-CT2001-00613.

REFERENCES

Abe, K., Jang, Y.J. and Leschziner, M.A., 2003, *Int. J Heat and Fluid Flow*, Vol.24, No.2 pp181-198.

Apsley, D.D. and Leschziner, M.A., 1998, *Int. J. Heat and Fluid Flow*, 19, 209-222.

Apsley, D.D. and Leschziner, M.A., 2000, *Flow, Turbulence and Combustion*, 63, pp81-112.

Betten, P., Craft, T.J., Leschziner, M.A. and Loyau, H. 1999, *J. AIAA*, 37, 785-796.

Chen, H.C., Jang, Y.J. and Han, J.H, 2000, *Int. J. Heat and Mass Transfer*, 43, 1603-1616.

Craft, T.J., 1998, *Int. J. Heat Fluid Flow*, 19, 541-548

Craft, T.J., and Launder, B.E. 1996, *Int. J. Heat Fluid Flow*, 17, 245.

Hanjalic, K. 1994, *Int. J. Heat Fluid Flow*, 15, 178-203

Jakirlic, S. and Hanjalic,. K., 1995, *Proc. 10th Symp. On Turbulent Shear Flows*, Pennsylvania State University, 23.25.

Jakirlic,S., Jester-Zuerker, R. and Tropea, C. (Eds.), 2001, *Proc. 9th ERCOFTAC/IAHR/COST Workshop on Refined Turbulence Modelling*, Darmstadt, October.

Jang, Y.J., Leschziner, M.A., Abe, K. and Temmerman, L., 2003, *Flow, Turbulence and Combustion* (in press).

Lien, F.S. and Leschziner, M.A., 1994, *Comput. Methods Appl. Mech. Engrg*, 114, pp123-148

Lien, F.S. and Leschziner, M.A., 1995, *The Aeronautical Journal*, 99, pp125-144

Lien, F.S. and Leschziner, M.A., 1997, *The Aeronautical Journal*, 101, pp269-275

May, N.E. 1999, *Engineering Turbulence Modelling and Experiments 4*, p329-338

Simpson, R.L., Long, C.H. and Byun, G., 2002, *Int. J. Heat and Fluid Flow*, 23, 582-591.

Speziale, C.G., Sarkar, S. and Gatski, T.B., 1991, *Journal of Fluid Mech.*, 227, 245-272.

Rodi, W., Bonnin, J-C., Buchal, P.,and Laurence, D., 1998, *EDF Report 98NB00004*

Temmerman, L., Leschziner, M.A., Mellen, C., and Frohlich, J. 2003, *Int. J. Heat and Fluid Flow*, 24(2), 157-180

Wallin, S. and Johansson, A.V.,2000 *Journal of Fluid Mech.*, 403, 89-132.

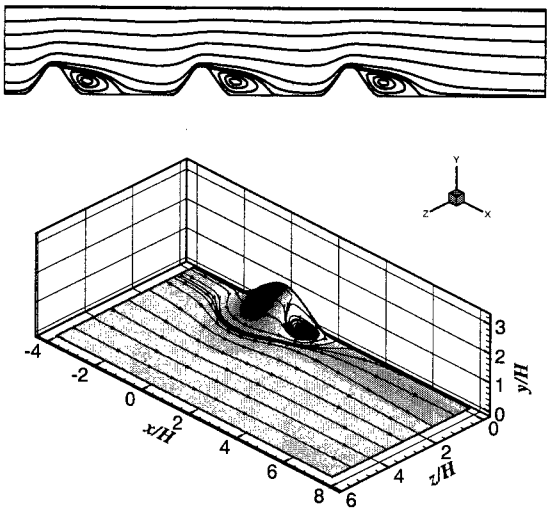

Fig. 1: geometries investigated

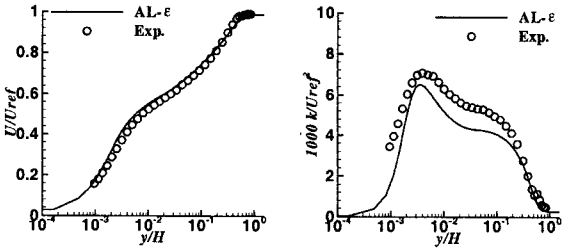

Fig. 2: Matching between the hill-free duct calculation and experiment.

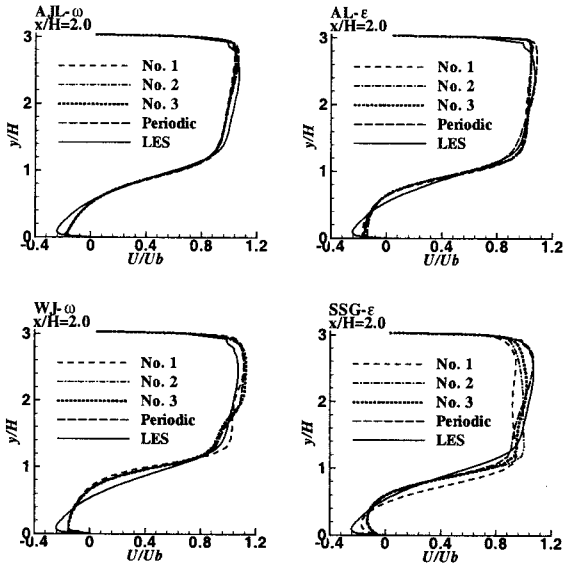

Fig. 3: Profiles of streamwise velocity at x/h=2.0

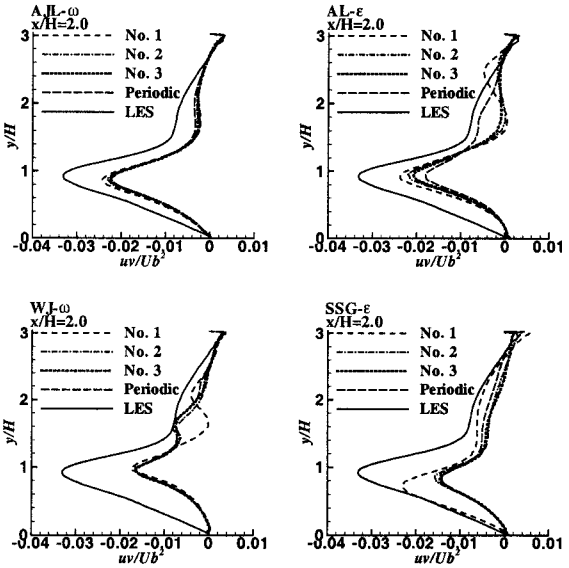

Fig. 4: Profiles of Reynolds shear stress at x/h=2.0

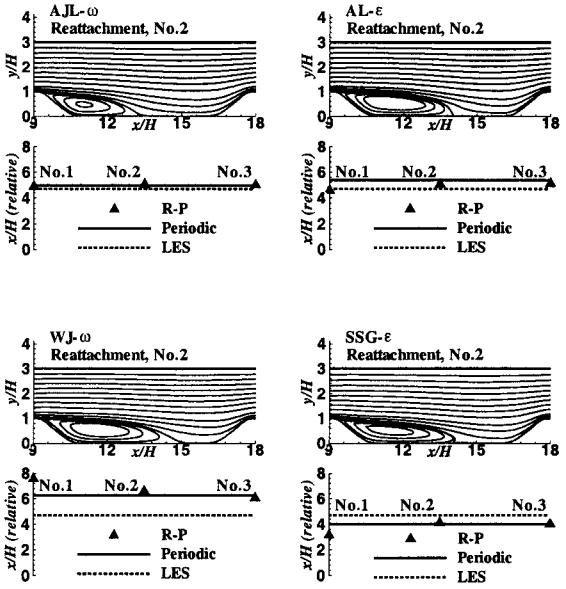

Fig.5 Streamfunction contours for hill 2 and related plots of hill-specific reattachment locations

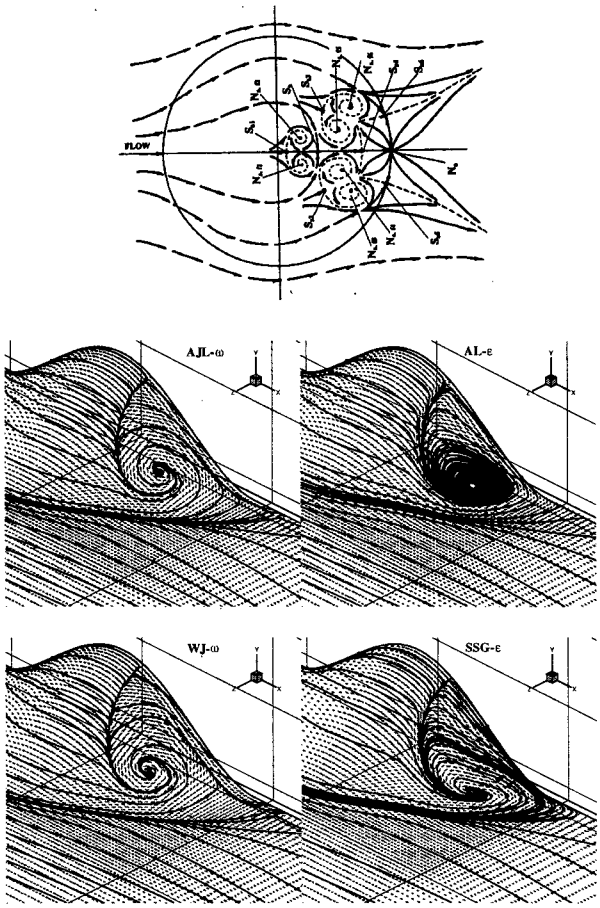

Fig. 6: Skin-friction lines on the hill surface

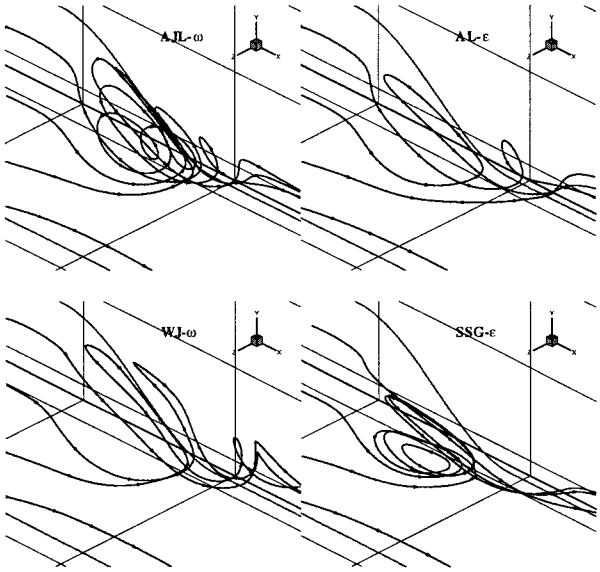

Fig. 7: Particle trace line predicted by models

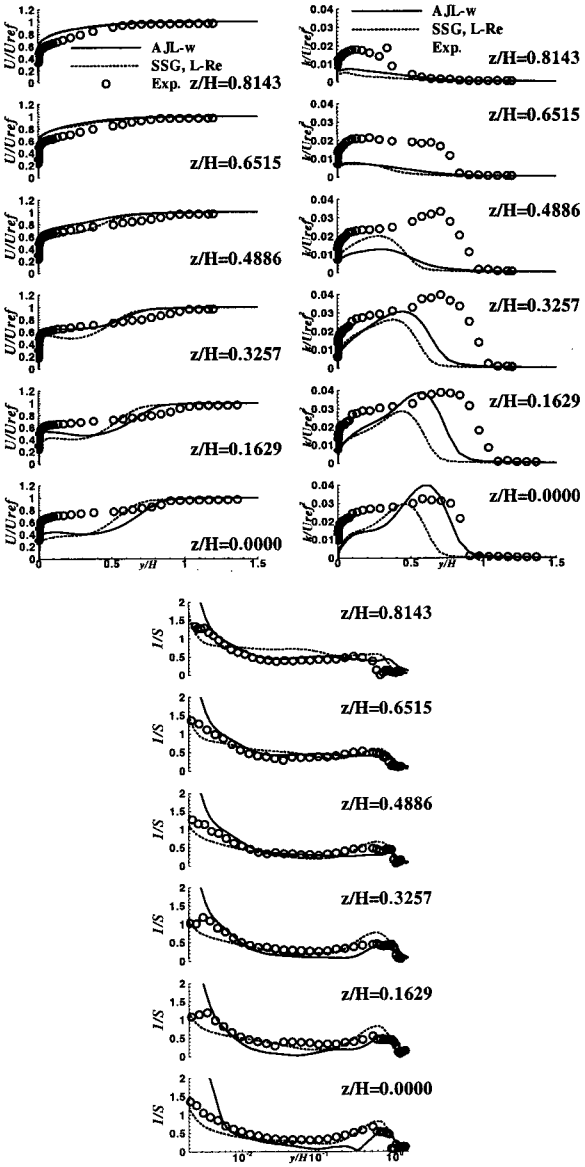

Fig. 8: Profiles of velocity, turbulence energy and parameter $1/S$ at x/H=3.63 and various spanwise localtions

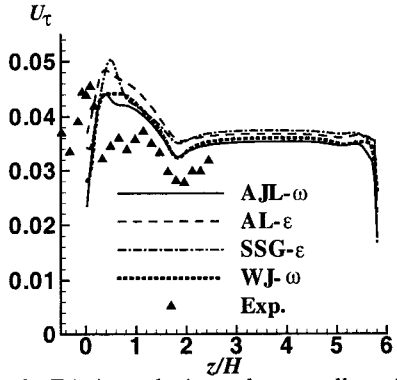

Fig. 9: Friction velocity on lower wall at x/H=3.63